JACS
JOURNAL OF THE AMERICAN CHEMICAL SOCIETY

Communication

pubs.acs.org/JACS

Proton Grease: An Acid Accelerated Molecular Rotor

Brent E. Dial, Perry J. Pellechia, Mark D. Smith, and Ken D. Shimizu*

Department of Chemistry and Biochemistry, University of South Carolina, Columbia, South Carolina 29208, United States

Supporting Information

ABSTRACT: A molecular rotor was designed that rotates 7 orders of magnitude faster upon protonation. The quinoline rotor is based on a rigid *N*-arylimide framework that displays restricted rotation due to steric interaction between the quinoline nitrogen and imide carbonyls. At rt (23 °C), the rotor rotates slowly ($t_{1/2}$ = 26 min, $\Delta G^{\ddagger}$ = 22.2 kcal/mol). However, upon addition of 3.5 equiv of acid the rotor rotates rapidly ($t_{1/2} = 2.0 \times 10^{-4}$ s, $\Delta G^{\ddagger}$ = 12.9 kcal/mol). Mechanistic studies show that this dramatic acid catalyzed change is due to stabilization of the planar transition state by the formation of an intramolecular hydrogen bond between the protonated quinoline nitrogen (N^{+}—H) and an imide carbonyl (O═C). The acid catalyzed acceleration is reversible and can be stopped by addition of base.

The development of new molecular devices is an active area of research due to their potential in electronics, catalysis, sensing, and nanotechnology applications.[1,2] One of the most common classes of molecular devices are molecular rotors, which convert kinetic, chemical, or photochemical energy into a circular motion.[3] The majority of stimuli−responsive rotors have been molecular brakes, which are slowed or stopped on application of a stimulus.[4] A greater challenge has been the development of rotors that rotate faster upon application of an external stimulus.[5]

Herein, we describe the design, synthesis, and study of a molecular rotor that rotates 10^7 times faster upon protonation (Scheme 1). The *N*-arylimide framework displays restricted rotation due to the steric repulsion between the quinoline nitrogen and imide carbonyls in the planar transition state (TS) where quinoline and succinimide rings are in alignment. Upon addition of acid, the rotor is able to form an intramolecular hydrogen bond in the TS, which greatly lowers the barrier of rotation. Thus, the protons, in this system, act as "molecular grease" that enables the quinoline nitrogen and imide carbonyls to slip by each other in the TS. This TS stabilizing mechanism contrasts with the ground state (GS) destabilizing mechanism of most stimuli-accelerated rotors.[5b,6]

Molecular rotor **1** is based on a rigid atropisomeric *N*-arylsuccinimide framework (Figure 1).[7] Restricted rotation around the central C_{aryl}–N_{imide} single bond leads to slow interconversion of enantiomeric rotamers at rt ($\Delta G^{\ddagger}$ = 22.2 kcal/mol, $t_{1/2}$ = 26 min). This atropisomeric framework has a number of attractive characteristics. (1) The highly hindered C_{aryl}–N_{imide} linkage is readily accessible via the thermal condensation of a hindered arylamine and cyclic anhydride.[8] (2) The rotational barriers can be tuned by variation of the number and size of the *ortho*-substituents on the arylamine.[9] (3) The 8-quinolyl nitrogen and imide carbonyl of rotor **1** are in perfect alignment to chelate a proton in the TS.[10] (4) Finally, the diastereotopic methyl groups of the succinimide ring provide a nice spectroscopic handle to monitor the rate of rotation via ^{1}H NMR.

Scheme 1. Acid−Base Equilibrium of an *N*-Aryl Imide Rotor (Top) and Transition States for the Rotation around the C_{aryl}–N_{imide} Bond (Bottom)[a]

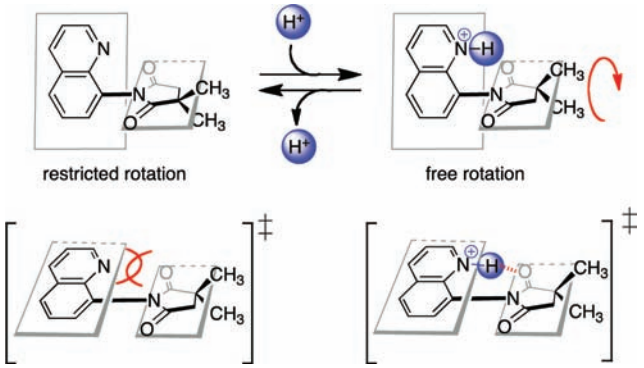

[a]Protonation of the quinoline nitrogen enables free rotation due to the formation of an intramolecular hydrogen bond.

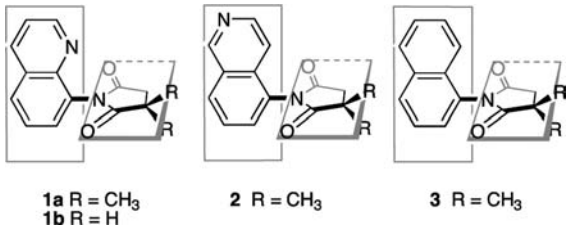

Figure 1. Quinoline rotor **1** and control rotors **2**−**3**.

Quinoline rotor **1** and control rotors **2** and **3** were prepared via neat thermal condensations of commercially available 2,2-dimethyl succinic anhydride with amino-quinoline, amino-isoquinoline, or 1-amino-naphthalene, respectively. The twisted structures of the rotors and the alignment of the imide carbonyl and quinoline nitrogen were confirmed by X-ray crystallographic studies of **1a** and **1b**-H^+ (Figure 2). For example, the quinoline and succinimide rings of **1a** are twisted out of plane with a dihedral angle of 87.9°, which is consistent with steric repulsion between the quinoline nitrogen and the imide carbonyls. The twisted conformation and slow rotation of **1a**

Received: December 23, 2011
Published: February 9, 2012

   dx.doi.org/10.1021/ja2120184 | *J. Am. Chem. Soc.* 2012, 134, 3675−3678

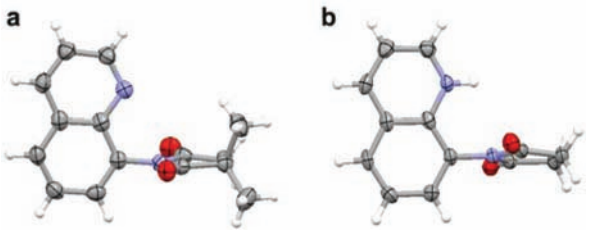

Figure 2. X-ray crystal structures of quinoline rotors **1a** and **1b**-H^+.

were also characterized in solution. In the ^{1}H NMR spectra, the methyl and methylene protons of the succinimide ring were diastereotopic at rt (Figure 3a, 0 equiv). The perpendicular *N*-

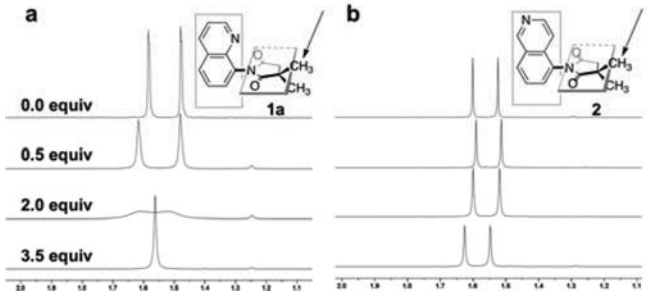

Figure 3. ^{1}H NMR spectra (TCE-d_2, 23 °C) of the diastereotopic methyl groups of rotor **1** and control **2** in the presence of 0.0, 0.5, 2.0, and 3.5 equiv of methanesulfonic acid.

quinolyl group desymmetrizes the top and bottom faces of the succinimide ring leading to well resolved singlets for the diastereotopic methyl groups in the ^{1}H NMR spectra.

The ability of acid to accelerate rotor **1** was first established via ^{1}H NMR titration of **1a** with methanesulfonic acid ($MeSO_3H$) in 1,1,2,2-tetrachloroethane-d_2 (TCE-d_2) at rt. Initially, the diastereotopic succinimide methyl groups were well resolved singlets (Figure 3a, 0 equiv). With the sequential addition of $MeSO_3H$, the rate of rotation increased dramatically, leading to broadening and coalescence of the diastereotopic methyl peaks. To confirm that coalescence was due to an increase in the rate of rotation and not to the acid–base equilibrium, ^{1}H NMR acid titrations were carried out using control rotors **2** and **3**.[4,5] Both control rotors have the same *N*-arylimide atropisomeric framework as **1** but are unable to form stabilizing hydrogen bonding interactions in their TSs due to the different position (rotor **2**) or the lack of a basic quinoline nitrogen (rotor **3**). The ^{1}H NMR spectra of the acid-titration experiments of the controls show some minor shifting and broadening, but the diastereomeric peaks do not coalesce (Figures 3b for **2** and S14 for **3**). These studies showed that the presence and positioning of the proton between the quinoline nitrogen and succinimide carbonyl were crucial for accelerating the rotational rate of rotor **1a**.

Free rotation in **1a**-H^+ can also be stopped by neutralization providing further evidence for the postulated mechanism. For example, serial addition of the base 2,6-lutidine to a solution of protonated rotor **1a** systematically reversed the broadening and coalescence of the diastereotopic methyl peaks (Figure S17). These qualitative protonation and deprotonation studies demonstrated that the rate of rotation of rotor **1a** can be dynamically controlled by the protonation state of the quinoline nitrogen.

Next, the influence of acid on the rates of rotation of rotors **1a**, **2**, and **3** were quantitatively assessed from their NMR measured rotational barriers (Figure 4). Due to the dramatic

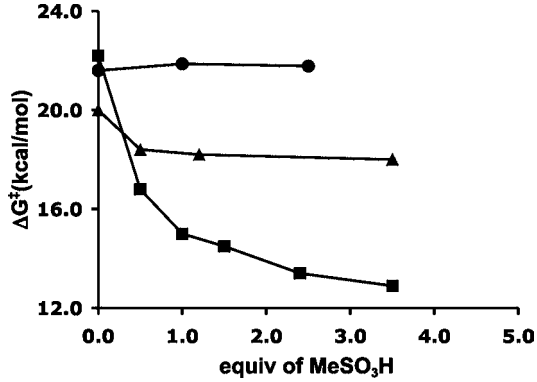

Figure 4. Rotational barriers of rotors **1a** and control rotors **2** and **3** (35 mM in TCE-d_2) in the presence of increasing number of equivalents of $MeSO_3H$. The barriers were measured via ^{1}H NMR by monitoring the methyl protons on the succinimide ring using 2D EXSY ($\Delta G^‡$ >19 kcal/mol) or VT ($\Delta G^‡$ < 19 kcal/mol).

difference in the rotational barriers of unprotonated and protonated rotor **1a**, the rotational barriers had to be measured by two methods. For barriers higher than 16 kcal/mol, the $\Delta G^‡$ were measured by two-dimensional exchange spectroscopy (2D EXSY NMR).[11] For barriers lower than 20 kcal/mol, the $\Delta G^‡$ were measured by variable temperature line shape analysis (VT NMR). The two methods provided consistent results, as barriers measured by both methods, in the overlap region (16.0–20.0 kcal/mol), had similar energies (±0.6 kcal/mol).

In the absence of acid, the rotational barriers of **1a**, **2**, and **3** were very similar at 20.0–22.2 kcal/mol (Figure 4, 0 equiv). With the addition of 3.5 equiv of $MeSO_3H$, a dramatic decrease in the rotational barrier of 9.3 kcal/mol was observed for rotor **1a**. The rotational barriers of the two control balances, in contrast, were relatively insensitive to changes in $MeSO_3H$ concentrations. For example, the rotational barrier of **2** decreased only 1.4 kcal/mol, and the barrier for **3** remained constant. The measured rotational barriers were also consistent with the previous qualitative studies. For example, the barrier of 22.2 kcal/mol for unprotonated **1a** corresponds to a rate that is slow on the NMR time scale (k_{rot} = 2.2 × 10^{-4} s^{-1}, $t_{1/2}$ = 26 min, at 23 °C) and fast for protonated **1a** (k_{rot} = 1700 s^{-1}, $t_{1/2}$ = 2.01 × 10^{-4} s, 3.5 equiv of $MeSO_3H$ at 23 °C). Although these barriers were measured at elevated temperatures, they can be used to accurately calculate rates of rotation at lower temperatures because the $\Delta G^‡$ for bond rotations have small entropic terms and, therefore, remain constant over a wide temperature range. Also, the rate of rotation, k_{rot}, was defined as half the measured rate of isomerization.[4c,f]

The asymptotic shape of the curve for **1a** in Figure 4 was consistent with that of a protonation process. However, the slope of the curve was more gradual than expected. Based on the large difference in pK_a's between $MeSO_3H$ and quinolinium (−1.9 and 4.9, respectively) a sharp break in the curve at 1.0 equiv was predicted. NMR titration of rotor **1a** in TCE confirmed that the quinoline nitrogen of the GS conformation was stoichiometrically protonated with 1 equiv of $MeSO_3H$ (Figure S18). Therefore, we propose that the need for excess $MeSO_3H$ to fully speed up rotation is due to the lower basicity

dx.doi.org/10.1021/ja2120184 | J. Am. Chem. Soc. 2012, 134, 3675–3678

of the quinoline nitrogen in **1a** in the sterically crowded planar TS.

Lastly, the mechanism of the proton accelerated rotation of **1** was studied. Specifically, the ability of protonated **1** to form an intramolecular hydrogen bond that stabilizes the TS was tested. First, the viability of the mechanism was examined by looking for similar examples in the literature. Two examples were found where chelation of a proton or metal ion by the planar TS significantly lowered the rotational barrier. Rebek et al. observed that the rotational barrier of chiral 2,2′-bipyridines decreased dramatically (>10 kcal/mol) upon binding a bridging $PdCl_2$ ion, which mediates the steric interactions between the opposing pyridine nitrogens in the planar TS.[12] More recently, Roussel et al. showed that *N*-aryl atropisomers similar in structure to rotor **1** had much lower rotational barriers when the ortho-aryl substituent could form a stabilizing intramolecular hydrogen bond in the TS.[13]

Experimental evidence of the proposed mechanism was found in the crystal structure of protonated **1b** (Figure 2b). This structure provides insight into the effects of protonating the quinoline nitrogen in the GS. The structure of **1b**-H^+ is virtually isostructural to that of **1a** and of unprotonated **1b** (Figure S20). For example, the quinoline and succinimide rings in the protonated **1b**-H^+ and unprotonated **1a** were nearly perpendicular with dihedral angles of 80° and 87.9°, respectively. More importantly, the proton on the quinoline nitrogen of **1b**-H^+ does not form any stabilizing intramolecular interactions with the opposing imide carbonyl. This confirms that the protonation of rotor **1** does not influence the GS structure. Therefore, by inference, the dramatically lower rotational barrier of protonated **1a**-H^+ must be due to changes in the structure and energy of the TS.

Molecular modeling studies also showed the viability of the proposed hydrogen bond stabilized TS in **1a**-H^+ (Figure 5).

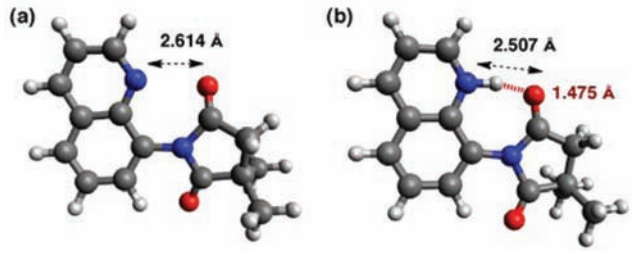

Figure 5. DFT B3LYP/6-311++G** optimized TS structures of (a) **1a** and (b) **1a**-H^+. The intramolecular N to O distances are highlighted in each structure. The TS of **1a**-H^+ forms a strong intramolecular hydrogen bond with a N^+–H•••O angle of 162.5° and a H•••O distance of 1.475 Å.

The energies and structures of the GS and TS of **1a** and **1a**-H^+ were calculated by DFT B3LYP/6-311++G**. The predicted GS and TS geometries of **1a** were in excellent agreement with the experimental values. The geometry of the calculated GS was twisted with a dihedral angel (88.6°) that was the same as that in the crystal structure (87.9°). The geometry of the calculated TS shows severe steric interactions between the quinoline nitrogen and imide carbonyls (Figure 5a) with an atom–atom distance (2.614 Å) that is well within the van der Waals radii of the atoms (3.07 Å). More importantly, an intramolecular N^+–H•••O hydrogen bond was formed in the TS of **1a**-H^+ (Figure 5b) with an unusually short H to O distance (1.475 Å).[14] The strong intramolecular hydrogen bond actually pulls the quinoline nitrogen and imide carbonyl closer together (2.507 versus 2.614 Å in **1a**) and allows them to pass more easily by each other in the TS.

The calculated rotational barriers from molecular modeling of the rotors were also in excellent agreement with the experimental values. For example, the difference in the calculated TS and GS energies of **1a** was 21.9 kcal/mol, which is very close to the experimental rotational barrier of 22.2 kcal/mol. Modeling also predicted that **1a**-H^+ had a significantly lower rotational barrier due to the formation of the strong ionic hydrogen bond in the TS. The only discrepancy was that the calculated barrier for **1a**-H^+ (5.05 kcal/mol) was much lower than the measured barrier (12.2 kcal/mol). This may be due to the ability of the solvent to stabilize the charge of **1a**-H^+ and reduce the strength of the intramolecular hydrogen bond in the experimental studies, whereas the theoretical studies were carried out *in vacuo*.[15]

The final observation in support of the proposed mechanism was evidence for the formation of similar stabilizing C–H•••O hydrogen bonds in the TSs of **2** and **3** that, likewise, lowers their rotational barriers. Rotors **2** and **3** have larger C–H groups at the 8-position in place of the smaller quinoline nitrogen of rotor **1a**. Therefore, we had expected that **2** and **3** would have higher rotational barriers than **1**. However, both the experimental (Figure 4) and computational studies were in agreement that **2** and **3** had equal or slightly lower rotational barriers than **1a**. For example, the measured rotational barriers of 20.0 and 21.6 kcal/mol for **2** and **3** were slightly lower than the measured barrier for **1a**, which was 22.2 kcal/mol. We attribute the lower than expected barriers of **2** and **3** to two factors: (1) the absence of lone pair–lone pair repulsive interactions between the quinoline nitrogen and imide carbonyl, in the planar TS and (2) the formation of attractive C–H•••O hydrogen bonds that stabilize the TSs of **2** and **3**. These interactions are isostructural with the proposed N^+–H•••O hydrogen bond in **1a**-H^+. However, these neutral hydrogen bonds in the TSs of **2** and **3** are much weaker, and thus their ability to lower the rotational barriers are much more modest.

In conclusion, a quinoline rotor with a rigid *N*-arylsuccinimide framework was designed in which rotation about the C_{ary}–N_{imide} bond is greatly accelerated by the addition of a proton guest. The protonation of the quinoline nitrogen reduces the steric repulsion in the TS leading to a lowering of the rotational barrier by 9.3 kcal/mol. Mechanistic studies confirmed that the operative mechanism involves the formation of a stabilizing intramolecular hydrogen bond between the imide carbonyl and protonated quinoline nitrogen in the coplanar TS. This system offers distinct advantages in that rotational motion of a molecular rotor is accelerated upon the addition of a proton or "molecular grease" and the protonation event is reversible allowing dynamic control over the rate of rotation. In future work, we hope to apply this system to the development of nanodevices or molecular sensors.

■ ASSOCIATED CONTENT

Ⓢ Supporting Information

Full experimental details of ^1H and ^{13}C NMR spectra, X-ray data, rotational barrier, and molecular modeling studies for compounds **1**–**3**. This material is available free of charge via the Internet at http://pubs.acs.org.

dx.doi.org/10.1021/ja2120184 | *J. Am. Chem. Soc.* 2012, 134, 3675–3678

AUTHOR INFORMATION

Corresponding Author

shimizu@mail.chem.sc.edu

Notes

The authors declare no competing financial interest.

ACKNOWLEDGMENTS

This work was supported by the National Science Foundation (CHEM 1112431).

REFERENCES

(1) (a) Leung, K. C.; Chak, C.; Lo, C.; Wong, W.; Xuan, S.; Cheng, C. H. K. *Chem.—Asian J.* **2009**, *4*, 364−381. (b) Gröger, G.; Meyer-Zaika, W.; Böttcher, C.; Gröhn, F.; Ruthard, C.; Schmuck, C. *J. Am. Chem. Soc.* **2011**, *133*, 8961−8971. (c) Stefankiewicz, A. R.; Tamanini, E.; Pantos, G. D.; Sanders, J. K. M. *Angew. Chem., Int. Ed.* **2011**, *50*, 5725−5728. (d) Landge, S. M.; Aprahamian, I. *J. Am. Chem. Soc.* **2009**, *131*, 18269−18271. (e) Zhang, D.; Zhang, Q.; Su, J.; Tian, H. *Chem. Commun.* **2009**, 1700−1702.

(2) (a) Balzani, V.; Credi, A.; Raymo, F. M.; Stoddart, J. F. *Angew Chem., Int. Ed.* **2000**, *39*, 3349−3391. (b) Balzani, V.; Credi, A.; Venturi, M. *Chem. Phys. Chem.* **2008**, *9*, 202−220. (c) Browne, W. R.; Feringa, B. L. *Nat. Nanotechnol.* **2006**, *1*, 25−35. (d) Kay, E. R.; Leigh, D. A.; Zerbetto, F. *Angew. Chem., Int. Ed.* **2007**, *46*, 72−191.

(3) (a) Kottas, G. S.; Clarke, L. I.; Horinek, D.; Michl, J. *Chem. Rev.* **2005**, *105*, 1281−1376. (b) Vacek, J.; Michl, J. *Adv. Funt. Mater.* **2007**, *17*, 730−739. (c) Kelly, T. R.; Sestelo, J. P.; Tellitu, I. *J. Org. Chem.* **1998**, *63*, 3655−3665. (d) Ghosn, M. W.; Wolf, C. *J. Org. Chem.* **2011**, *76*, 3888−3897. (e) Spivey, A. C.; Zhu, F.; Mitchell, M. B.; Davey, S. G.; Jarvest, R. L. *J. Org. Chem.* **2003**, *68*, 7379−7385. (f) Clayden, J.; Fletcher, S. P.; McDouall, J. J. W.; Rowbottom, S. J. M. *J. Am. Chem. Soc.* **2009**, *131*, 5331−5343.

(4) (a) Jog, P. V.; Brown, R. E.; Bates, D. K. *J. Org. Chem.* **2003**, *68*, 8240−8243. (b) Basheer, M. C.; Oka, Y.; Mathews, M.; Tamaoki, N. *Chem.—Eur. J.* **2010**, *16*, 3489−3496. (c) Yang, J. S.; Huang, Y. T.; Ho, J. H.; Sun, W. T.; Huang, H. H.; Lin, Y. C.; Huang, S. J.; Huang, S. L.; Lu, H. F.; Chao, I. *Org. Lett.* **2008**, *10*, 2279−2282. (d) Zhang, D.; Zhang, Q.; Sua, J. H.; Tian, H. *Chem. Commun.* **2009**, 1700−1702. (e) Rebek, J. Jr.; Trend, J. E.; Wattley, R. V.; Chakravorti, S. *J. Am. Chem. Soc.* **1979**, 4333−4337. (f) Yang, C.; Prabhakar, C.; Huang, S.; Lin, Y.; Tan, W. S.; Misra, N. C.; Sun, W.; Yang, J. *Org. Lett.* **2011**, *13*, 5632−5635.

(5) (a) Dial, B. E.; Rasberry, R. D.; Bullock, B. N.; Smith, M. D.; Pellechia, P. J.; Profeta, S. Jr; Shimizu, K. D. *Org. Lett.* **2011**, *13*, 244−247. (b) Alfonso, I.; Burguete, M. I.; Luis, S. V. *J. Org. Chem.* **2006**, *71*, 2242−2250. (c) Welch, C. J.; Biba, M.; Pye, P.; Angelaud, R.; Egbertson, M. *J. Chromatogr., B* **2008**, *875*, 118−121.

(6) Schoevaars, A. M.; Kruizinga, W.; Zijlstra, R. W. J.; Veldman, N.; Spek, A. L.; Feringa, B. L. *J. Org. Chem.* **1997**, *62*, 4943−4948.

(7) (a) Pais, V. F.; Remon, P.; Collado, D.'; Andreasson, J.; Perez-Inestrosa, E.; Pischel, U. *Org. Lett.* **2011**, *13*, 5572−5575. (b) Curran, D. P.; Geib, S.; DeMello, N. *Tetrahedron* **1999**, *55*, 5681−5704.

(8) (a) Lavin, J. M.; Shimizu, K. D. *Chem. Commun.* **2007**, *3*, 228−230. (b) Degenhardt, C.; Lavin, J.; Smith, M.; Shimizu, K. *Org. Lett.* **2005**, *7*, 4079−4081. (c) Rasberry, R. D.; Wu, X.; Bullock, B. N.; Smith, M. D.; Shimizu, K. D. *Org. Lett.* **2009**, *11*, 2599−2602.

(9) (a) Rasberry, R. D.; Shimizu, K. D. *Org. Biomol. Chem.* **2009**, *7*, 3899−3905. (b) Kishikawa, K.; Yoshizaki, K.; Kohmoto, S.; Yamamoto, M.; Yamaguchi, K.; Yamada, K. *J. Chem. Soc., Perkin Trans. 1* **1997**, 1233−1239. (c) Verma, S. M.; Singh, N. B. *Aust. J. Chem.* **1976**, *29*, 295−300.

(10) Spivey, A. C.; Charbonneau, P.; Fekner, T.; Hochmuth, D. H.; Maddaford, A.; Malardier-Jugroot, C.; Redgrave, A. J.; Whitehead, M. A. *J. Org. Chem.* **2001**, *66*, 7394−7401.

(11) (a) Perrin, C. L.; Dwyer, T. J. *Chem. Rev.* **1990**, *90*, 935−967. (b) Ernst, R. R. *Principles of Nuclear Magnetic Resonance in One and Two Dimensions*; Claredon Press: Oxford, 1987; pp 326−328.

(12) Rebek, J.; Costello, T.; Wattley, R. V. *Tetrahedron Lett.* **1980**, *21*, 2379−2380.

(13) Roussel, C.; Vanthuyne, N.; Bouchekara, M.; Djafri, A.; Elguero, J.; Alkorta, I. *J. Org. Chem.* **2008**, *73*, 403−411.

(14) (a) Smith, G; Wermuth, U. D.; White, J. M. *Acta Crystallogr., Sect. C* **2008**, *64*, 180−183. (b) Dobosa, R.; Osmialowski, B.; Gawinecki, R. *Struct. Chem.* **2010**, *21*, 1037−1041.

(15) Chen, J.; McAllister, M. A.; Lee, J. K.; Houk, K. J. *J. Org. Chem.* **1998**, *63*, 4611−4619.